International Journal of Food Microbiology 407 (2023) 110420

Contents lists available at ScienceDirect

International Journal of Food Microbiology

journal homepage: www.elsevier.com/locate/ijfoodmicro

Synthesis of silver nanoparticles using *Bacillus velezensis* M3-7 lipopeptides: Enhanced antifungal activity and potential use as a biocontrol agent against Fusarium crown rot disease of wheat seedlings

Fatma Masmoudi [a,*], Nandagopal S. Pothuvattil [b], Slim Tounsi [c], Imen Saadaoui [a,d], Mohamed Trigui [e]

[a] Biotechnology Program, Center of Sustainable Development, College of Art and Sciences, Qatar University, P.O. Box 2713, Doha, Qatar
[b] Central Laboratories Unit (CLU), Qatar University, P.O. Box 2713, Doha, Qatar
[c] Laboratory of Biopesticides (LBPES), Center of Biotechnology of Sfax, Sfax University, Sfax, Tunisia
[d] Department of Biological and Environmental Sciences, College of Art and Sciences, Qatar University, P.O. Box 2713, Doha, Qatar
[e] Laboratory of Environmental Sciences and Sustainable Development (LASED) Sfax Preparatory Engineering Institute, BP 1172-3018, University of Sfax, Tunisia

ARTICLE INFO

Keywords:
Antifungal activity
B. velezensis
FCR disease
Lipopeptides
Silver nanoparticles
Wheat

ABSTRACT

Bacillus velezensis M3-7 is a hyperactive mutant, 12-fold improved in its antifungal activity, obtained during a previous study from the wild strain BLB371 after a combination of random mutagenesis and medium component optimization. This study explores the use of this mutant in synthesizing silver nanoparticles (Ag-NPs) for the control of Fusarium crown rot disease (FCR) in wheat seedlings. LC-MS/MS analysis proved that both strains co-produced different families of lipopeptides and that mutagenesis caused the hyper-production of iturin A C14 and C15, the liberation of iturin A C10 and C12, and the inhibition of fengycin release. Our aim was a further improvement in the antifungal activity of the wild strain and the mutant M3-7 in order to control Fusarium crown rot disease (FCR) in wheat seedlings. Therefore, a nanotechnology approach was adopted, and different lipopeptide concentrations produced by the wild strain and the mutant M3-7 were used as capping agents to synthesize silver nanoparticles (Ag-NPs) with enhanced antifungal activity. Ag-NPs formed using 3 $mg{\cdot}mL^{-1}$ of the mutant lipopeptides were found to exhibit a good distribution, improved antifungal activity, a promising potential to be used as a biofortified agent for seed germination, and an effective compound to control FCR in wheat seedlings.

1. Introduction

Phytopathogenic microorganisms, including bacteria, fungi, and viruses, present a real threat to various plant crops causing crucial agricultural losses worldwide (John et al., 2021), which in turn threaten food security. Fungi are the main cause of plant diseases and yield loss. They can attack plants in pre-harvest as well as post-harvest processes, affect various plant varieties, colonize all plant tissues and soils, and lead to an annual economic loss exceeding 200 billion USD (Horbach et al., 2011).

Phytopathogenic fungi are responsible for various crop diseases. They are well known for their high virulence, plant growth disruption, hormone imbalances, leaf epinasty, root branching, and other symptoms. (John et al., 2021). Besides, fungi, such as *Aspergillus* species, produce highly toxic, hallucinogenic, and carcinogenic substances that are harmful to human health (Pankaj et al., 2018).

A number of strategies have been developed management fungal disease propagation and reduce their dramatic impacts on agricultural products. Chemical fungicides are the most commonly used products. However, the systematic and extensive use of these synthetic compounds can impose some concerns due to the emergence of resistance in the pathogen, the lack of effective products against the target fungal agent, and the adverse effects on human health and environmental balance (Carvalho, 2017). This critical situation has stimulated many research efforts to develop sustainable strategies to maintain soil fertility and improve yields. The use of plant growth promoting bacteria (PGPB), especially those belonging to the *Bacillus* genus, has been investigated as a promising alternative to control and manage fungal diseases

* Corresponding author at: Centre for Sustainable Development, College of Arts and Sciences, Qatar University, P.O. Box 2713, Doha, Qatar.
E-mail address: fatma.masmoudi@qu.edu.qa (F. Masmoudi).

https://doi.org/10.1016/j.ijfoodmicro.2023.110420
Received 3 June 2023; Received in revised form 23 September 2023; Accepted 27 September 2023
Available online 28 September 2023

(Masmoudi et al., 2017; Zouari et al., 2020). In fact, *Bacillus* species such as *B. velezensis* (formerly named *B. amyloliquefaciens* subsp. *plantarum*) are described for their capacity to produce non-ribosomally synthesized cyclic lipopeptides (LPs) (Meena and Kanwar, 2015; Toral et al., 2018) composed of a hydrophilic peptide part and a hydrophobic alkyl chain lipopeptide (Hutchinson et al., 2017). *Bacillus* lipopeptides may be classified in three main families; surfactins, iturins, and fengycin (Hutchinson et al., 2017). Surfactins and iturins are heptapeptides. The iturin group comprises seven variants, including Bacillomycins and Mycosubtilins. Fengycins A and B, also called plipastatins, are lipodecapeptides. Lipopeptides are potent biosurfactants mainly responsible for antagonism towards phytopathogens and plant disease reduction (Torres et al., 2016). They are nontoxic, highly biodegradable, stable, tolerant to different temperatures and pH, and nonpolluting biomolecules (Hutchinson et al., 2017; Meena and Kanwar, 2015).

The different families of lipopeptides are usually known to act synergistically to enhance antagonistic activities (Tanaka et al., 2015). Besides their antagonistic properties, LPs are also involved in root colonization as well as in the systemic stimulation of the plant immune system (Henry et al., 2011; Malviya et al., 2020). Despite the fact that lipopeptides have many advantages over chemical products, the main drawback limiting industrial-scale lipopeptide production and purification is their high cost (Mnif and Ghribi, 2015). Several studies proposed various methods to reduce secondary metabolite production costs, including the use of cheaper raw materials or agro-industrial waste products, statistical optimization of production, and strain mutation to improve metabolite release (Masmoudi et al., 2017; Umar et al., 2021). With the emergence of the nanotechnology sciences, increasing efforts are focused on the synthesis of nanoparticles (NPs) using lipopeptides as capping agents (Ravi et al., 2021). The antimicrobial properties of NPs such as chitosan, iron oxide, silica, silver, zinc oxide, and aluminosilicates have already been reported. These activities vary according to the size, surface structure, surface charge, and extent of aggregation or disaggregation of each particle (Parveen et al., 2018; Pillai et al., 2020). For instance, silver nanoparticles are well known for their low toxicity to humans and animals as well as their efficiency in boosting yields and controlling plant diseases (Hashem et al., 2021). Therefore, various efforts have been focused on expanding the antimicrobial expression of lipopeptides by nanosupplementation. This technique will be useful not only to overcome the costly manufacture problem of lipopeptides but also to sustain agricultural practices thanks to the stability, dispersions, and effectiveness of these compounds in controlling pathogens (Ravi et al., 2021).

Accordingly, the goal of this research was to improve the antifungal activity of the mutant *Bacillus velezensis* M3-7 using the nanotechnology sciences. This strain was generated on the basis of the wild strain *Bacillus velezensis* BLB371 using a combination of two methods: mutagenesis and medium component optimization. When compared to the wild strain, the mutant exhibited 12-fold improved antifungal activity against several phytopathogenic fungi and presented a high efficacy in protecting post-harvested tomato fruits against gray mold disease (Masmoudi et al., 2017). In this current study, ***(i)*** both strains, *B. velezensis* BLB371 (the wild strain) and *B. velzensis* M3-7 (the mutant), were checked for their production of lipopeptides using ribosomal gene detection and LC-MS/MS analysis. ***(ii)*** Silver nanoparticles (Ag-NPs) were synthesized using different concentrations of lipopeptide extracts as capping agents, then studied by transmission electron microscopy (TEM). ***(iii)*** The synthetized Ag-NPs were evaluated for their antifungal activities, phytotoxicity, and ability to inhibit Fusarium crown root disease (FCR) in wheat seedlings.

2. Materials and methods

2.1. Microorganisms and growth conditions

The *B. velezensis* BLB371 belongs to the bacterial strain collection of the Biopesticides Laboratory of the Center of Biotechnology of Sfax (CBS), and it was isolated from a Tunisian soil. The optimal biosynthesis of lipopeptides of this strain was carried out in the optimized medium MC (pH 7.0), which contained: 25 g L^{-1} sucrose, 20 g L^{-1} peptone, 4.5 g L^{-1} yeast extract, 2 g L^{-1} KH_2PO_4, 0.6 g L^{-1} $MgSO_4$, and 6 mg L^{-1} $MnSO_4$ (Mezghanni et al., 2012). The hyperactive mutant strain M3–7 has been obtained by random mutagenesis from the wild strain BLB371, and its optimized lipopeptide production medium contains: 35 g L^{-1} peptone, 32.5 g L^{-1} sucrose, 10.5 g L^{-1} yeast extract, 2.4 g L^{-1} KH_2PO_4, 1.3 g L^{-1} $MgSO_4$, and 23 mg L^{-1} $MnSO_4$ (Masmoudi et al., 2017).

2.2. Production and preparation of crude lipopeptides

The lipopeptides were extracted using an acidic method, where the cell-free supernatant of the BLB371 or M3–7 strain was acidified with hydrochloric acid to a pH of 2. The obtained precipitate was extracted with methanol, and the obtained solvent was evaporated to dryness using a rotary vacuum evaporator. The crude extract was dissolved in tris-HCl buffer (50 mM, pH 7.5), filtered through 0.22 μm filters, and stored at 4 °C for further experimentation.

2.3. PCR detection of lipopeptides and polyketides biosynthesis genes

After genomic DNA extraction, PCR amplifications were performed with the following cycle conditions: an initial denaturation step at 95 °C for 3 min, followed by 35 cycles of denaturation at 95 °C for 45 s, 1 min for primer annealing at 46 to 62 °C, and 72 °C extension for 40 s, followed by a final extension step for 7 min at 72 °C. Primer pairs used in the PCR amplifications of lipopeptides and polyketides biosynthesis genes are mentioned in Table 1. After PCR amplification, 5 μL of each reaction was visualized on an agarose gel (1 %) using the electrophoresis technique. When amplicons of the expected sizes appeared, PCR was scored positive (Frikha-Gargouri et al., 2017).

2.4. Isolation and identification of lipopeptides using LC-MS/MS analysis

Potential lipopeptides existing in each crude extract of the wild strain *B. velezensis* BLB371 and the mutant M3-7 were analyzed and compared using an Agilent 1100 LC system consisting of a degasser, binary pump, auto sampler, and column heater. The column outlet was coupled to an Agilent MSD ion trap XCT mass spectrometer equipped with an ESI ion source. Metabolite identification and mass spectrometric evaluation were performed using a single quadrupole mass detector (SQD), by setting the electrospray ionization conditions in the MS and detecting the mass of molecular ions (Ben Abdallah et al., 2015). For the chromatographic separation, a Zorbax 300 Å Extend-C-18 column (4.6 × 250 mm) and a linear gradient of water and acetonitrile were used. During the elution program, a flow rate of 0.4 mL/min was applied, and the injection volume of 20 μL was used for sample introduction. The detection was performed using the positive/alternating ion mode. The column was held at 75 % solvent A (water) and 25 % solvent B (acetonitrile) for 4 min, followed by a 14 min step gradient from 25 % B to 100 % B, then it was kept at 100 % B for 6 min, and subsequently, the elution was achieved with a linear gradient from 100 % B to 25 % B in 8 min. Pure lipopeptides such as iturin and fengycin were used as reference to identify the lipopeptides of the crude extract based on the similarity of their retention in addition to their molecular weight.

2.5. Synthesis of silver nanoparticles (Ag-NPs)

Silver nanoparticles (Ag-NPs) with improved antifungal activity were synthesized using silver nitrate ($AgNO_3$) and various concentrations of lipopeptides (3, 6, and 10 mg·mL^{-1}) extracted from the wild strain BLB371 and the mutant M3-7. Each lipopeptide solution was subjected to bath sonication at 4 °C for 30 min. Next, $AgNO_3$ solution (1 mM) was slowly added dropwise to the lipopeptide solution. The

Table 1
Primers for PCR detection of lipopeptide and polyketide biosynthesis genes in *B. velezensis* BLB371 and M3–7.

	Primers	Sequences of primers for PCR product	Size (bp)	Annealing temperature (°C)	Reference
Surfactin	SFP-F	5′-ATGAAGATTTACGGAATTTA	675	46	Chung et al., 2008
	SFP-R	5′-TTATAAAAGCTCTTCGTACG			
Fengycin	FENB-F	5′CCTGGAGAAAGAATATACCGTACCY	670	53	Chung et al., 2008
	FENB-R	5′-GCTGGTTCAGTTKGATCACAT			
	FEND-F	5′-GGCCCGTTCTCTAAATCCAT	269	55	Mora et al., 2011
	FEND-R	5′-GTCATGCTGACGAGAGCAAA			
Iturin	ITUC-F	5′-CCCCCTCGGTCAAGTGAATA	594	62	Chung et al., 2008
	ITUC-R	5′-TTGGTTAAGCCCTGATGCTC			
	ITUD-F	5′-TTGAAYGTCAGYGCSCCTTT	482	60	
	ITUD-R	5′-TGCGMAAATAATGGSGTCGT			
Bacillomycin	BMYB-F	5′-GAATCCCGTTGTTCTCCAAA	370	55	Chung et al., 2008
	BMYB-R	5′-GCGGGTATTGAATGCTTCTT			
Macrolactin	mlnA-F	5′-CCGTGATCGGACTGGATGAG	668	58	Compaoré et al., 2013
	mlnA-R	5′-CATCGCACCTGCCAAATACG			
Bacillaen	baeA-F	5′-ATGTCAGCTCAGTTTCCGCA	688	58	Compaoré et al., 2013
	baeA-R	5′-GATCGCCGTCTTCAATTGCC			
Difficidin	dfnA-F	5′-GGATTCAGGAGGGCATACCG	653	58	Compaoré et al., 2013
	dfnA-R	5′-ATTGATTAAACGCGCCGAGC			

reaction mixture was then incubated on a rotary shaker at 40 °C and 200 rpm for 48 h during which the solution turned dark in color, indicating the formation of Ag-NPs. The prepared nanoparticles were centrifuged at 13,500*g* for 15 min, washed using demineralized water and then dried in a hot air oven at 45 °C. The Ag-NPs product was then stored in a refrigerator at 4 °C until further analysis.

2.6. Transmission electron microscopy (TEM) analysis

Ag-NPs solutions were first centrifuged at 13,500*g* for 15 min to obtain the crude sample for TEM analysis. The samples were then diluted and dispersed in isopropanol using a bath sonicator for 20 min. Next, 1 μL of the dispersed solution was drop-cast onto an agar-carbon film 300 copper mesh and left to dry before being analyzed using a FEI Tecnai G2 S-Twin 200 kV FEG Transmission Electron Microscope.

2.7. Antifungal activity measurement

The antifungal activity of the synthesized Ag-NPs against *Fusarium culmorum* ISPAVE21w, a phytopathogenic fungus responsible for FCR in wheat seedlings, was evaluated. The evaluation included determining the inhibition zones (IZ) on potato dextrose agar (PDA), as well as assessing the minimum inhibitory concentrations (MIC) and minimal fungicidal concentrations (MFC) using 96-well microplates (Masmoudi et al., 2017). All plates were incubated at 27 °C for 3 days. MIC was determined as the minimum concentration of Ag-NPs that inhibited any visible growth. The MFC was defined as the lowest concentration of Ag-NPs that killed >99.9 % of the original inoculum (Trigui et al., 2013).

2.8. Plant bioassays

The study aimed to evaluate the potential phytotoxicity and phytostimulation effects of the synthesized Ag-NPs. Durum wheat seeds (*Triticum durum* L. var. *Karim*) were surface sterilized using 5 % bleach and 70 % ethanol followed by washes using sterile distilled water and then divided into five groups for germination tests. The first three groups were incubated for 120 min in 1 mg·mL^{-1} of ***(i)*** the nanoparticle suspension formed using 3 mg·mL^{-1} of mutant lipopeptides as a capping agent (Ag-M3), ***(ii)*** the M3–7 lipopeptides crude suspension (LPM3), and ***(iii)*** the commercial chemical fungicide Uniform® 446SE. After incubation, all seeds were transplanted into pots (5 seeds per pot) and inoculated with *F. culmorum* spore suspension (10^5 spores·mL^{-1}). Seeds incubated in distilled water and not inoculated with the fungal spore suspension were considered the positive control, and seeds incubated in distilled water and inoculated with the fungal spore suspension were used as the negative control. Each treatment consisted of three pots, and the pots were arranged in a randomized block design and kept for 2 weeks at room temperature under 16 h of light and 8 h of darkness at 27 °C. Seedlings were daily irrigated with autoclaved distilled water and the germination rate, plant height, crown root incidence, and plant protection were recorded and calculated at the end of the experiment as follow (Naseri and Marefat, 2011; Wildermuth et al., 1997):

Germination rate (%)
= ((Total number of seeds − Germinated)/Total number of seeds tested)*100

Plant protection (%) = ((Total number of obtained seedlings − FCR infected seedlings)/Total number of obtained seedlings)*100

CRI (%) = $(2N_1 + 5N_2 + 10N_3,)$*100/(10*Total number of obtained seedlings)

Where $\boldsymbol{N_1}$, is the number of plants presenting crown rot in the sub-crown internodes <25 %, $\boldsymbol{N_2}$ is the number of plants presenting crown rot in the sub-crown internodes between 25 and 50 %, and $\boldsymbol{N_3}$ is the number of plants presenting crown rot in the sub-crown internodes >50 %.

2.9. Statistical analysis

The Statistical Package for the Social Sciences (SPSS V.11; SPSS Inc., Chicago, IL, USA) was adopted for the analysis of variance. Mean values among treatments at the 5 % level of significance ($p = 0.05$) were compared using the Duncan's multiple range test.

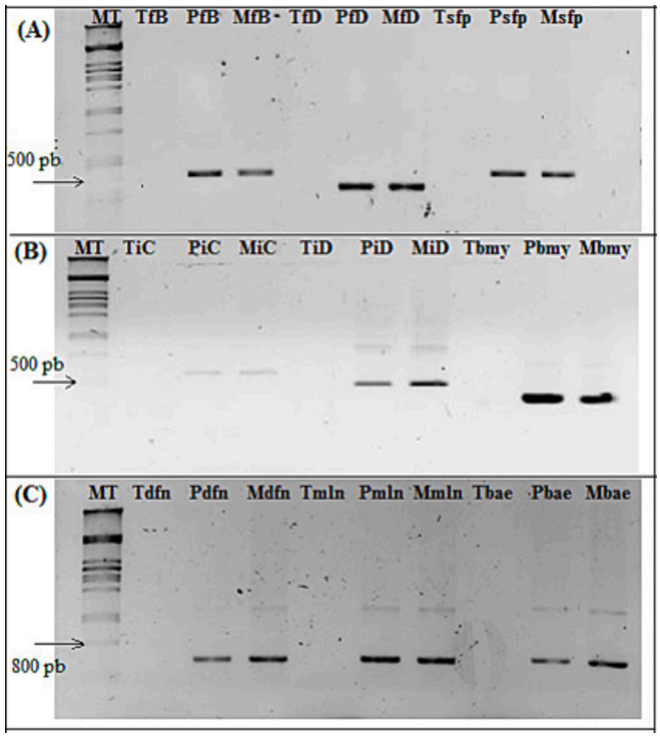

Fig. 1. PCR amplification and comparison of lipopeptide and polyketide genes in *B. velezensis* BLB371 and the Mutant M3–7. **(A)**: PCR amplification of fengycin and surfactin genes; **(B)**: PCR amplification of Iturin and bacillomycin genes; **(C)**: PCR amplification of polyketides genes; **MT**: λpst DNA Ladder (Promega); **TfB, TfD, Tsfp TiC, TiD, Tbmy, Tdfn, Tmln** and **Tbae**: negative control of fenB, fenD, sfP, ituC, ituD, bmyB, Difficidin, macrolactin and Bacillaene genes, respectively; **PfB, PfD, Psfp, PiC, PiD, Pbmy, Pdfn, Pmln** and **Pbae**: PCR amplification of fenB, fenD, sfP, ituC, ituD, bmyB, Difficidin, macrolactin and Bacillaene genes, respectively, in the parent strain BLB371; **MfB, MfD, Msfp, MiC, MiD, Mbmy, Mdfn, Mmln** and **Mbae**: PCR amplification of fenB, fenD, sfP, ituC, ituD, bmyB, Difficidin, macrolactin and Bacillaene genes, respectively, in the mutant strain M3–7.

3. Results

3.1. PCR detection of non-ribosomal lipopeptides and polyketides synthetase

During this study, the PCR method was used to detect of key biosynthetic genes, shedding light on the potential co-production capabilities of the wild strain *B. velezensis* BLB371 and the mutant M3–7 in relation to diverse antifungal lipopeptides and polyketides. A total of nine non-ribosomal lipopeptide synthetase genes (fenB, fenD, sfP, ituC, ituD, bmyB, Difficidin, macrolactin and Bacillaene) were efficiently amplified and amplicons with the expected sizes were obtained through the implementation of the designated primer pairs (Fig. 1). This outcome distinctly demonstrated that both the wild-type and mutant strains shared an identical biosynthetic gene profile. Specifically, each strain harbored unique genes (fenB, fenD, sfP, ituC, and ituD) contributing to the synthesis of three distinct families of lipopeptides (iturin, fengycin, and surfactin) (Fig. 1(A)). Furthermore, these strains featured different genes (Difficidin, macrolactin, and Bacillaene) associated with the production of polyketides such as difficidin, macrolactin, and bacillaene (Fig. 1(C)).

3.2. LC-MS/MS comparison of lipopeptides pattern produced by B. velezensis BLB371 and the mutant M3-7 in vitro

The production of lipopeptides was verified through the characterization and comparison of the lipopeptide pattern of the *B. velezensis* wild strain BLB371 and the mutant M3–7 using specific LC-MS/MS methods. As anticipated, most of the identified peaks from both varieties were lipopeptidal in nature (mass ≈1000 m/z). Nevertheless, there were differences in the generated metabolites (Fig. 2). The mutant M3–7 efficiently co-produced Iturin and Surfactin families of lipopeptides, with sets of mass peaks detected within each family, with an interval of 14 and with different numbers of methylene groups (-CH2-) in fatty acyl chains (Ben Abdallah et al., 2015). The wild strain BLB371 efficiently

Table 2
Lipopeptide produced by *B. velezensis* BLB371 and the mutant M3–7 as detected by LC-MS/MS.

Lipopeptide family	Molecular mass [M-H]-	Assignment		References
		BLB371 extract	M3-7 extract	
Iturin A	986,48	–	C10	(Price et al., 2007)
Iturin A	1014,51	–	C12	(Price et al., 2007)
Iturin A	1040,9	C14	C14	(Malfanova et al., 2012)
Iturin A	1054,7	C15	C15	(Malfanova et al., 2012)
Surfactin	1020	C14	C14	(Malfanova et al., 2012)
Surfactin	1033,9	C15	C15	(Malfanova et al., 2012)
Fengycin A	1474.8	C17	–	(Malfanova et al., 2012)
Fengycin B	1521.22	C18	–	(Malfanova et al., 2012)

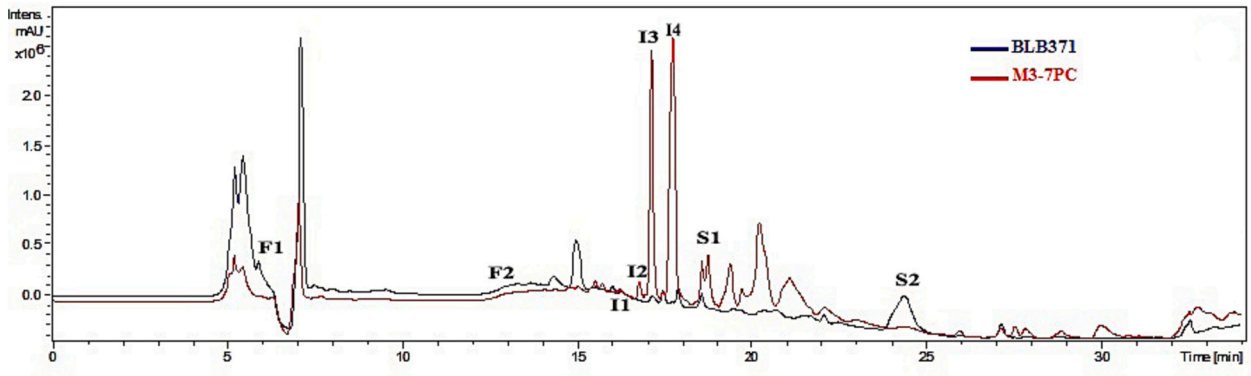

Fig. 2. Comparison of LC-MS/MS separation profiles between the wild strain BLB371 and the mutant M3–7. **F1**: Fengycin A C17; **F2**: Fengycin B C18; **I1**: Iturin A C10; **I2**: Iturin A C12; **I3**: Iturin A C14; **I4**: Iturin A C15; **S1**: Surfactin C14; **S2**: Surfactin C15.

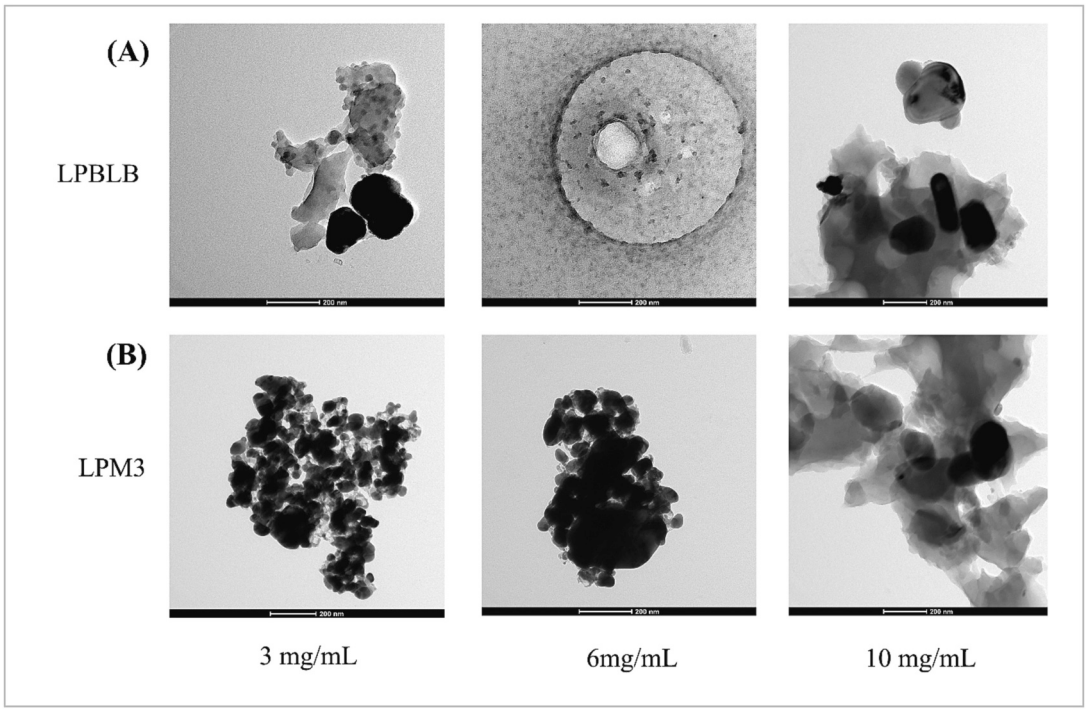

Fig. 3. Transmission electron microscopy images of the formed Ag-NPs using different concentrations the lipopeptides biosynthesized by *B. velezensis* 371 **(A)** and the mutant *B. velezensis* M3–7 **(B)**. **LPBLB**: lipopeptides produced by BLB371; **LPM3**: lipopeptides produced by the mutant M3–7.

secreted all three families of lipopeptides: Iturin, Fengycin and Surfactin. It releases Fengycin A C17 (m/z = 1474.8) and Fengycin B C18 (m/z = 1521.22), Iturin A C14 and C15, and Surfactin C14 and C15 (Table 2). Although the wild strain produced Fengycin, which is known to be an efficient inhibitor of fungus proliferation, the mutant M3–7 exhibited the most significant antifungal activity. LC-MS/MS profiles of the mutant and parent strains revealed that BLB371 had low production of lipopeptides which proved that in the case of the strain M3–7 the genome shuffling affected the specific pathways responsible for the production of Iturin A C10 and C12, while improving the production of Iturin A C14 and C15, and inhibiting Fengycin release (Fig. 2).

3.3. Characterization of Ag-NPs

TEM analysis was used to confirm the formation of Ag-NPs by examining their shape and morphology. The figures obtained after TEM analysis (Fig. 3(A)) clearly show that the concentration of BLB 371 lipopeptides at 6 mg·mL^{-1} allowed the synthesis of Ag-NPs with a very good distribution and spherical shape. However, the nanoparticles aggregated excessively at both BLB lipopeptide (LPBLB) concentrations of 3 and 10 mg·mL^{-1}, which could disrupt the structure of the peptides and may reduce the antifungal activity. When using increasing concentrations of LPM3 (3 and 6 mg·mL^{-1}), the synthesis of the Ag-NPs was enabled, and the obtained compounds exhibited a good distribution. However, at a concentration of 10 mg·mL^{-1}, the formed particles had poor distribution, which could affect the compound's structure and efficiency (Fig. 3(B)).

3.4. Antifungal activity assessment

Compounds formed with silver ions have the potential to act as hazardous elements for various phytopathogenic fungi. In order to study the *in-vitro* antifungal activity of our synthesized Ag-NPs, it is mandatory to compare the inhibiting potential of the formed lipopeptide-conjugated Ag-NPs against the free form of the pure lipopeptidic extracts of both strains (LPBLB and LPM3). Therefore, we studied the ability of all obtained compounds to inhibit the growth of the phytopathogenic fungus *F. culmorum*.

Table 3
Ag-NPs potentialities to inhibit *F. culmorun* proliferation.

		3 mg·mL^{-1}	6 mg·mL^{-1}	10 mg·mL^{-1}
LPBLB	I.Z (mm)	0	9 ± 0.7	12 ± 0
	MIC (mg·mL^{-1})	4 ± 1.7		
	MFC (mg·mL^{-1})	>6		
LPM3	I.Z (mm)	10.5 ± 0.7	13.5 ± 0.7	22.5 ± 0.7
	MIC (mg·mL^{-1})	0.5 ± 0.21		
	MFC (mg·mL^{-1})	2 ± 0.86		
Ag-BLB	I.Z (mm)	19 ± 0	26.5 ± 0.71	9 ± 0
	MIC (mg·mL^{-1})	1.5 ± 0	0.625 ± 0.21	1.66 ± 0.72
	MFC (mg·mL^{-1})	>3	1.5 ± 0	5 ± 0
Ag-M3	I.Z (mm)	28.5 ± 0.71	39.5 ± 0.71	15 ± 0
	MIC (mg·mL^{-1})	0.375 ± 0	0.155 ± 0.05	0.9 ± 0.39
	MFC (mg·mL^{-1})	0.625 ± 0.21	0.5 ± 0.21	5 ± 0

I.Z: diameter of the inhibition zone; **MIC**: minimum inhibitory concentration; **MFC**: minimum fungicidal concentration; **Ag-BLB**: Ag-LPs synthetized with BLB371 lipopeptides. **Ag-M3**: Ag-LPs synthetized with M3-7 lipopeptides; **LPBLB**: Pure lipopeptides extracted from the strain BLB371; **LPM3**: Pure lipopeptides extracted from the mutant M3-7.

The inhibition zones (in mm) of the different concentrations of lipopeptides and Ag-NPs samples were given in Table 3. The antifungal activity of LPM3 extracts was higher than that of LPBLB extracts. The inhibitory potential of LPM3 increased with initial concentrations and reached 22.5 ± 0.7 mm at a concentration of 10 mg·mL^{-1}, while that of LPBLB was around 12.0 ± 0 mm at the same concentration (Table 3).

When capped with silver ions, Ag-NPs compounds showed outstanding antifungal efficacy. Likewise, Ag-NPs made with the mutant lipopeptides showed the highest antifungal activity compared to Ag-NPs synthesized with the wild strain lipopeptides. However, this activity varied depending on the initial concentration of the pure lipopeptidic extract. For example, Ag-NPs synthetized using 3 and 6 mg·mL^{-1} of LPM3, exhibited significant antifungal activity against *F. culmorum* with an inhibition zone of 28.5 ± 0.71 mm and 39.5 ± 0.71 mm, respectively.

In contrast, Ag-NPs synthesized with 3 and 6 mg·mL^{-1} of LPBLB had less effective antifungal activity with an inhibition zone which of 19 ± 0 and 26.5 ± 0.71 mm, respectively. Moreover, the antifungal activity of both synthesized Ag-BLB and Ag-M3 decreased to 9 and 15 mm, respectively, using a concentration of 10 mg mL^{-1}.

The antifungal activity of synthetized Ag-NPs was quantified using the 96-well micro-plates method by measuring the minimal inhibitory concentration (MIC), and minimal fungal concentrations (MFC) (Table 3). The MIC and MFC results were consistent with those obtained using the inhibition zone. The Ag-M3 compound demonstrated potent antifungal activities with a low MIC concentration of (0.155 ± 0.05 mg·mL^{-1}), which was three time better than the pure lipopeptide extract (0.5 ± 0.21 mg·mL^{-1}). The MFC was 0.5 ± 0.21 mg·mL^{-1} compared to 2 ± 0.86 mg·mL^{-1} for the pure extract LPM3 (Table 3). Therefore, synthetized Ag-M3 with a concentration of 3 mg·mL^{-1} of lipopeptide extract exhibited a fungicidal effect (MFC/MIC ≤ 2), whereas LPM3 pure lipopeptide has a fungistatic potential (MFC/MIC > 2).

3.5. Effect of Ag-NPs treatment on Fusarium crown rot disease (FCR)

As a first step, the phytotoxicity of Ag-M3 was assessed *in-vivo* on wheat seeds. Interestingly, as indicated by the Duncan test, seeds treated with LPM3 or Ag-M3 then exposed to *F. culmorum* attack (LPM3 + Fc and AgM3 + Fc, respectively), exhibited significant differences in germination rates and displayed an enhanced phytostimulation potential ($p < 0.05$) in comparison to the two control groups (UT + water and UT + Fc) (Fig. 4). These findings highlight the lipopeptides' phytostimulatory impact, negate any phytotoxic impact of our synthesized Ag-M3 and instead demonstrate its ability to stimulate plant growth.

The assessment of Ag-M3's ability to manage FCR disease in wheat seedlings and its comparison with LPM3 and the commercial pesticide Uniform® was performed by subjecting treated and untreated seedlings to a two-week monitoring of their growth and development under fungus attack. Results showed that among the treated groups, seedlings treated with Ag-M3 displayed the most improved physiological characteristics, such as plant height, growth, and root architecture and development (Fig. 5(A)).

Plant height measurements revealed a significant improvement in seedling height with the application of Uniform®, LPM3 or the synthesized Ag-M3 ($p < 0.5$) (Fig. 5(B)). This improvement can be attributed to the better protection against *F. culmorum* attack, which caused severe crown rot symptoms in the non-treated plants (NT + Fc) and reduced their growth compared to the positive control (NT + water) (Fig. 5(C) and (D)).

In fact, seeds treated with Ag-M3, LPM3, or Uniform ® and exposed to fungus attack displayed reduced severity levels with a protection percentage exceeding 80 %. In contrast, the non-treated control subjected to fungal attack (NT + FC) exhibited protection below 40 %, with the highest crown rot incidence (CRI) reaching 72 % (Fig. 5(C) and (D)).

Interestingly, the greatest reduction in FCR was noted after the treatment with M3-Ag, showcasing plant protection surpassing 96 % and a minimal CRI of nearly 7 % (Fig. 5(D)). These experiments highlight the enhanced protective potential of Ag-M3 synthesized nanoparticle, positioning them as a promising biofungicide against various fungal diseases particularly, FCR.

4. Discussion

Durum wheat is a is an economically important crop worldwide and is critical to global food security (Acevedo et al., 2018). However, it is highly susceptible to several foliar and root diseases, especially Fusarium crown rot caused by *F. culmorum* (Chekali et al., 2011). Therefore, improving the wheat's resistance to antifungal attacks is a priority for sustaining food security. The synthesis of an ecofriendly biofungicide with a high performance is highly requested to decrease the resistance of fungi to conventional fungicides. In a previous study by Masmoudi et al. (2017), the mutant *B. velezensis* M3–7, obtained from the parent strain BLB371 after a combination of random mutagenesis and medium component optimization, exhibited improved antifungal activity against several phytopathogenic fungi among them *Fusarium* species.

In the initial stage of this research, we aimed to prove that the improvement of antifungal activity observed in the mutant M3–7 is mainly related to an improvement in quantities and qualities of produced cyclic lipopeptides. Genome shuffling and optimization of the composition of the culture medium can have a significant impact on the nature and the concentrations of lipopeptides produced by microorganisms (Xia and Wen, 2022). Thus, the lipopeptide and polyketide synthetase genes of both the parent strain BLB371 and the mutant M3–7 were analyzed using genetic markers and LC-MS/MS method. The results showed that both strains BLB371 and M3–7 possessed the same non ribosomal peptide synthetase genes involved in the production of lipopeptides and we detected amplicons with expected sizes and with all the genetic markers used. Our findings are consistent with previous studies that have demonstrated the presence of different genes responsible for the production of the three families of lipopeptides in *Bacillus velezensis* (formerly known as *B. amyloliquefaciens* subs. *plantarum*) (Ben Abdallah et al., 2015; Frikha-Gargouri et al., 2017).

Using LC coupled to mass spectrometry, we found that the parent

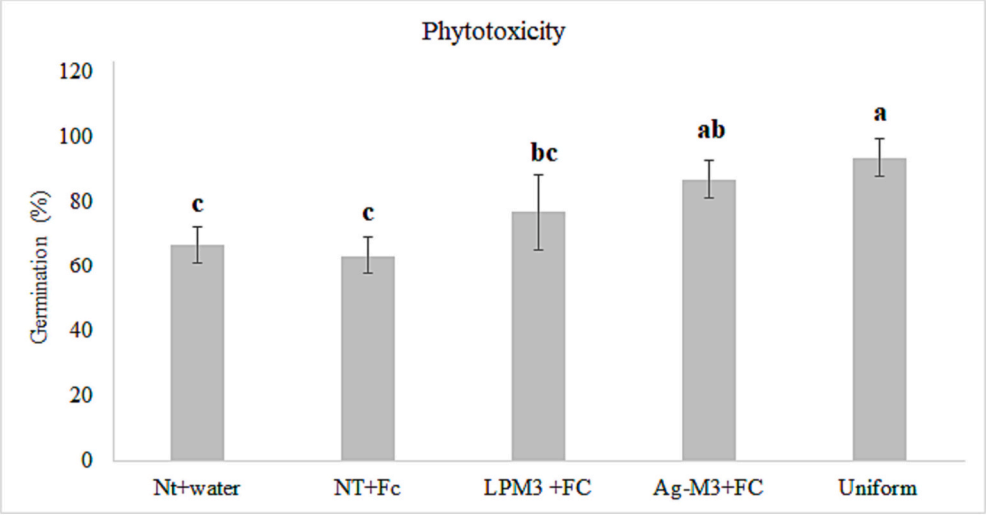

Fig. 4. Phytotoxicity/ phytostimulation effect of Ag-M3 treatments on seed germination.

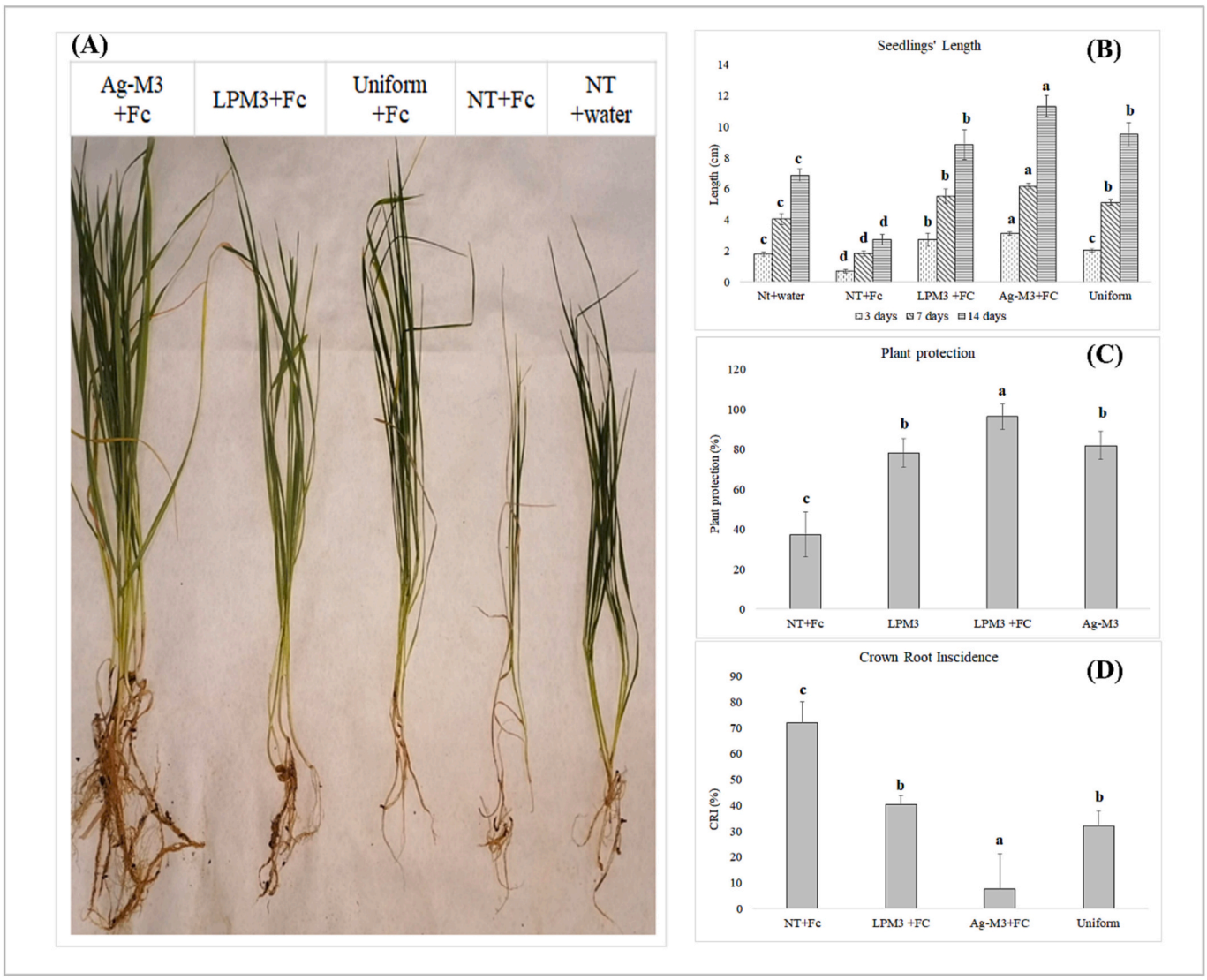

Fig. 5. Efficiency of Ag-M3 compounds to control FCR disease by improving seedling development **(A)** and height **(B)** under fungus attack, improving plant protection **(C)** and inhibiting crown rot incidence **(D)**.

strain BLB371 co-produced a wide variety of lipopeptides. Isoforms of Surfactins (C14 and C15), Iturins A (C14 and C15) as well as Fengycins A (C17) and B (C18) were detected according to the mass spectra. However, the mutant M3–7 was only able to produce two families of lipopeptides: surfactins (C10, C12, C14 and C15), iturins (C14 and C15). Notably, no peak grouping in the mass range of the fengycin family was detected. As the mutant M3–7 was generated through three rounds of classic mutagenesis (Masmoudi et al., 2017). The conjunction of several findings lent weight to the hypothesis that genome shuffling may have played a role in instigating the observed differences between the parent and mutant strains. Classic mutagenesis is a random process, affecting various pathways simultaneously which result in simultaneous changes in the production of various metabolites. Mutations induced by random mutagenesis have the potential to influence multiple regulatory elements, modify the expression levels of specific enzymes involved in the biosynthetic pathways of lipopeptides, and impact transcription factors or signaling pathways associated with biosynthesis (Wu et al., 2014). This complex and multifaceted mechanisms may lead to phenomena such as stimulation, hyper-production, or downregulation.

In our study, the detection of fengycin in the wild strain, the successful detection of the fenD gene linked to fengycin production through PCR screening in both strains, and the absence of the corresponding peak of these compounds by LC-MS/MS in the mutant provided initial support to the notion that genome shuffling disrupted the pertinent pathways for the synthesis of this lipopeptide.

Our hypothesis is supported by some similar observations previously reported in the literature. For instance, while several biosynthetic operons were detected, the corresponding antibiotics were not found in the extracts (Athukorala et al., 2009; Dimkić et al., 2017). Yaseen et al. (2018) explained that a decrease in fengycin production observed in the parental strain of *B. subtilis* might be linked to a genome shuffling of the pnpA gene. Nevertheless, in our case, to firmly establish the validity of this hypothesis, it is imperative to undertake further investigations primarily genome sequencing. Such an investigation would definitively ascertain the genomic changes that underlie the altered lipopeptide profiles.

The strong antifungal activity characterizing the mutant M3–7 could be attributed to the presence of iturins A, which are known to be efficient antifungal compounds (Kim et al., 2020; Yan et al., 2020; Yaseen et al., 2018). LC-MS/MS showed that the homologs of iturins were not distributed the same way among the two types of crude extracts from both strains. In LPM3, we noted the appearance of iturins A C10 and C12, in addition to the amelioration of peaks corresponding to iturins A C14 and C15, suggesting that this compound was most abundant in the

mutant extract compared with the same compound present in the wild strain extract.

All of these results have been reported in the literature. Kim et al. (2020) proved that the higher antifungal activity of the mutant *B. velezensis* against *F. oxysporum* resulted from the increased expression of biosynthesis genes associated with iturin production. Dimkić et al. (2017) also reported that extracts with the highest concentrations of iturin achieved the strongest inhibitory effect against fungal proliferation. From their side, Shi et al. (2018) declared that two rounds of genome shuffling enhanced the yield of iturin A produced by *B. amyloliquefaciens* LZ-5 by two-fold. Moreover, the results of LC-MS/MS analysis revealed a significant the improvement in the production of surfactin isoforms in the mutant strain M3–7, indicating that genome shuffling may enhance metabolic capability, gene expression, and function related to surfactin synthesis (Kim et al., 2020; Zhao et al., 2014). Compared to the wild strain BLB371, the mutant M3–7 produced a greater variety and higher concentrations of surfactin isoforms which may explain the improved antifungal activity of M3–7. Although this lipopeptide alone exhibited weak activity against fungal aggressors (Alvarez et al., 2012; Kim et al., 2020), it can synergistically interact with iturin A isoforms and enhance their antifungal activity (Kim et al., 2020; Li et al., 2023). Moreover, surfactin promotes root tissue colonization, alters membrane integrity, and contributes to the release of antifungal substances (Cawoy et al., 2015). Taken together, these findings suggest that the improved antifungal activity of M3–7 could be attributed to the upregulation of iturin and surfactin biosynthesis genes and the enhanced production of iturin and surfactin metabolites. Our results demonstrate that mutagenesis affected multiple lipopeptide production pathways, resulting in increased surfactin production, hyper-production of iturin A C14 and C15, and inhibition of fengycin release.

Lipopeptides are safe and highly efficient molecules in the treatment of cryptogamic diseases which preserve plant growth and yield and contribute to the improvement of food security. However, their production processes are often expensive. Therefore, it is crucial to find ways to improve the efficiency of these compounds even in small doses, and develop a more affordable and effective biofungicide for the treatment of diseases such as FCR. Synthesis of metallic nanoparticles associated with lipopeptides as capping agents could be a potential solution which can provide an eco-friendly and cost-effective biofungicide. Given that the wild strain *B. velezensis* BLB371 and the mutant M3–7 produce different families and isoforms of lipopeptides, we aimed to synthesize Ag-LPs using different concentrations of the crude extract from both strains. Results obtained through TEM analysis showed that the lipopeptide concentration and composition in the crude extract significantly influenced the morphology, distribution, and size of Ag-NPs. The most efficient concentration to obtain Ag-NPs with good distribution and spherical shape was found to be 6 $mg{\cdot}mL^{-1}$ of BLB371 lipopeptides. However, for mutant lipopeptides, concentrations of 3 and 6 $mg{\cdot}mL^{-1}$ were considered the most efficient for synthesizing Ag-NPs with good distribution. These findings are consistent with previous reports in the literature, which have shown that lipopeptide concentrations and forms have significant impacts on the size, uniformity, distribution, and stability of the synthesized nanoparticles (Bezza et al., 2020; Rangarajan et al., 2018). As mentioned above, lipopeptides produced by the mutant M3–7 contained higher levels of iturin when compared those produced by the wild strain. Some previous report have suggested that iturin's functional groups such as hydroxyl, carboxyl, and phenolic groups can react with heavy metals (Zhang et al., 2016; Zhao et al., 2019). Iturin is also known for its cyclic structure made up of 7 amino acids (Zhao et al., 2019) that could play a crucial role in enhancing Ag-NPs formation These amino acids may play an important role to improve Ag-NPs formation (Chandra and Singh, 2018). Therefore, we can assume that when lipopeptides contain higher concentrations in iturin played important roles in stabilization of Ag-NPs which justify our findings that lipopeptides produced by our mutant M3–7 lead to the synthesis of an Ag-NPs with a good distribution and using lower concentration of crude extract.

Regarding the antifungal activity, Ag-M3 exhibited an improved antifungal activity with a MIC of 0.155 ± 0.05 $mg{\cdot}mL^{-1}$and MFC of 0.5 ± 0.21 $mg{\cdot}mL^{-1}$. Ag-M3 synthetized using a concentration of 3 $mg{\cdot}mL^{-1}$ of lipopeptide extract showed a fungicidal effect, while the pure LPM3 pure lipopeptide exhibited fungistatic potential (MFC/MIC > 2). These results are consistent with previous studies that have shown the effectiveness of lipopeptide-synthesized nanoparticles in enhancing antifungal activity and suppressing fungal plant diseases (Lin et al., 2020; Ravi et al., 2021). Additionally, Ibrahim et al. (2020) demonstrated that the growth of the phytopathogenic fungus *F. graminearum* was strongly suppressed regardless of the concentration of the synthesized AgNPs.

In another part of our study, we aimed to investigate the improvement of the *in-vivo* phytostimulation efficiency of our synthesized Ag-LPs, as well as their enhanced potential to inhibit *F. culmorum* proliferation and eradicate FCR disease in wheat seedlings.

Wheat seeds treated with LPM3 or Ag-M3 and subsequently exposed to fungal attack demonstrated a significant and equivalent improvement in germination rates, resulting in enhanced phytostimulation potential when compared to untreated seeds. This improvement in seed germination can be attributed to the involvement of lipopeptides in eradicating *Fusarium* proliferation and providing crucial protection against Damping off disease. Our findings align with prior studies that have highlighted the high capacity of free cell extracts derived from *Bacillus* species to stimulate seed germination (Masmoudi et al., 2019). For instance, Yánez-Mendizábal and Falconí (2018) evidenced the potential role of lipopeptides produced by *Bacillus* spp. in controlling anthracnose and improving germination in *Andean lupin* seeds.

Regarding the protection of wheat seedlings from FCR disease, it is indeed accurate that treatment with LPM3 presented a strong potential to protect wheat seedlings against FCR disease, aligning with well-established findings in existing literature. For instance, Li et al. (2022) reported the significant biocontrol capacity of lipopeptides produced by *B. halotolerans* QTH8 in combating wheat crown rot. Additionally, Taheri et al. (2023) highlighted the antagonistic effects of lipopeptides from *Bacillus subtilis* CB2, contributing to the suppression of *Fusarium graminearum* on the heads and crowns of susceptible wheat varieties. Interestingly, the application of synthesized Ag-M3 nanoparticles yielded substantial enhancements in plant height, root architecture, plant protection, and the suppression of crown rot incidence (CRI), surpassing the effects of treatment with LPM3 or Uniform®. Few previous studies have investigated the effect of conjugated nanoparticles and lipopeptides in *in-vivo* studies. For example, Panichikkal et al. (2021) showed the ability of *B. licheniformis* encapsulated in alginate-chitosan nanoparticle beads supplemented with rice starch to enhance *Capsicum annuum* (*L.*) (chilli) germination and protect seedlings from fungal disease caused by *Sclerotium rolfsii.* Mittal et al. (2022) found that green silver nanoparticles prepared by *Bacillus* sp. GP23 inhibited the growth of the pathogenic fungus *Fusarium oxysporum* and controlled the adverse effects on chickpea seedlings.

To the best of our knowledge, this is the first study to extrapolate the beneficial effect of Ag-LPs on wheat seedlings and their effectiveness against FCR disease. These experiments confirmed the obtained results, qualifying M3-Ag as a promising biofungicide against various fungal diseases, mainly FCR.

5. Conclusion

This study evidenced the high ability of the hyperactive mutant *B. velezensis* M3–7 to produce lipopeptides such as Iturin and Surfactin. These M3–7 lipopeptides were employed for the synthesis of Ag-NPs to control and eradicate FCR disease. The co-production of important concentrations and different families of lipopeptides by the mutant M3–7 allowed for the successful synthesis of Ag-M3 with a good

distribution and a potent fungicidal effect against *F. culmorum*. Moreover, the Ag-M3 compound demonstrated its potential as a phytostimulator agent for wheat seed germination and proved to be an effective nano-biopesticides against FCR diseases. Finally, the use of nano-biofungicides synthesized using microbial lipopeptides can offer several advantages over traditional chemical-based agents, including improved control efficiency, reduced industrial costs, and an excellent sustainable candidate for plant stress management.

CRediT authorship contribution statement

Fatma Masmoudi: Conceptualization, Methodology, Formal analysis, Investigation, Writing – original draft. **Nandagopal S. Pothuvattil:** Methodology, Software, Data curation. **Slim Tounsi:** Conceptualization, Resources, Writing – review & editing, Funding acquisition. **Imen Saadaoui:** Conceptualization, Writing – review & editing, Visualization, Project administration. **Mohamed Trigui:** Conceptualization, Methodology, Validation, Data curation, Writing – review & editing, Visualization, Supervision.

Declaration of competing interest

The authors declare that they have no conflict of interests regarding the present study.

Data availability

Data will be made available on request.

Acknowledgements

This work was supported by grants from the Tunisian Ministry of Higher Education and Scientific Research. This research was supported in part by the Centre for Sustainable Development, Qatar University. TEM analysis was accomplished in the Central Laboratories unit, Qatar University. The statements made herein are solely the responsibility of the authors. Open Access funding provided by the Qatar National Library.

References

Acevedo, M., Zurn, J., Molero, G., Kumar Singh, P., He, X., Aoun, M., Juliana, P., Bockleman, H., Bonman, M., El-Sohl, M., Amri, A., Coffman, R., McCandles, L., 2018. The Role of Wheat in Global Food Security, pp. 81–110. https://doi.org/10.4324/9780203733301-4.

Alvarez, F., Castro, M., Príncipe, A., Borioli, G., Fischer, S., Mori, G., Jofré, E., 2012. The plant-associated *Bacillus amyloliquefaciens* strains MEP218 and ARP23 capable of producing the cyclic lipopeptides iturin or surfactin and fengycin are effective in biocontrol of sclerotinia stem rot disease. J. Appl. Microbiol. 112, 159–174. https://doi.org/10.1111/j.1365-2672.2011.05182.x.

Athukorala, S.N., Fernando, W.D., Rashid, K.Y., 2009. Identification of antifungal antibiotics of *Bacillus* species isolated from different microhabitats using polymerase chain reaction and MALDI-TOF mass spectrometry. Can. J. Microbiol 55 (9), 1021–1032. https://doi.org/10.1139/W09-067.

Ben Abdallah, D., Frikha-Gargouri, O., Tounsi, S., 2015. *Bacillus amyloliquefaciens* strain 32a as a source of lipopeptides for biocontrol of *Agrobacterium tumefaciens* strains. J. Appl. Microbiol. 119, 196–207. https://doi.org/10.1111/jam.12797.

Bezza, F.A., Tichapondwa, S.M., Chirwa, E.M.N., 2020. Synthesis of biosurfactant stabilized silver nanoparticles, characterization and their potential application for bactericidal purposes. J. Hazard. Mater. 393, 122319 https://doi.org/10.1016/j.jhazmat.2020.122319.

Carvalho, F.P., 2017. Pesticides, environment, and food safety. Food Energy Secur. 6, 48–60. https://doi.org/10.1002/fes3.108.

Cawoy, H., Debois, D., Franzil, L., De Pauw, E., Thonart, P., Ongena, M., 2015. Lipopeptides as main ingredients for inhibition of fungal phytopathogens by *Bacillus subtilis/amyloliquefaciens*. J. Microbial. Biotechnol. 8, 281–295. https://doi.org/10.1111/1751-7915.12238.

Chandra, A., Singh, M., 2018. Biosynthesis of amino acid functionalized silver nanoparticles for potential catalytic and oxygen sensing applications. Inorg. Chem. Front. 5, 233–257. https://doi.org/10.1039/C7QI00569E.

Chekali, S., Gargouri, S., Paulitz, T., Nicol, J.M., Rezgui, M., Nasraoui, B., 2011. Effects of *Fusarium culmorum* and water stress on durum wheat in Tunisia. Crop Prot. 30, 718–725. https://doi.org/10.1016/j.cropro.2011.01.007.

Chung, S., Kong, H., Buyer, J.S., Lakshman, D.K., Lydon, J., Kim, S.-D., Roberts, D.P., 2008. Isolation and partial characterization of *Bacillus subtilis* ME488 for suppression of soilborne pathogens of cucumber and pepper. Appl. Microbiol. Biotechnol. 80, 115–123. https://doi.org/10.1007/s00253-008-1520-4.

Compaoré, C.S., Nielsen, D.S., Ouoba, L.I.I., Berner, T.S., Nielsen, K.F., Sawadogo-Lingani, H., Diawara, B., Ouédraogo, G.A., Jakobsen, M., Thorsen, L., 2013. Co-production of surfactin and a novel bacteriocin by *Bacillus subtilis* subsp. *subtilis* H4 isolated from Bikalga, an African alkaline *Hibiscus sabdariffa* seed fermented condiment. Int. J. Food Microbiol. 162, 297–307. https://doi.org/10.1016/j.ijfoodmicro.2013.01.013.

Dimkić, I., Stanković, S., Nišavić, M., Petković, M., Ristivojević, P., Fira, D., Berić, T., 2017. The profile and antimicrobial activity of *Bacillus* lipopeptide extracts of five potential biocontrol strains. Front. Microbiol. 8.

Frikha-Gargouri, O., Ben Abdallah, D., Ghorbel, I., Charfeddine, I., Jlaiel, L., Triki, M.A., Tounsi, S., 2017. Lipopeptides from a novel *Bacillus methylotrophicus* 39b strain suppress *Agrobacterium* crown gall tumours on tomato plants. Pest Manag. Sci. 73, 568–574. https://doi.org/10.1002/ps.4331.

Hashem, A.H., Abdelaziz, A.M., Askar, A.A., Fouda, H.M., Khalil, A.M.A., Abd-Elsalam, K.A., Khaleil, M.M., 2021. *Bacillus megaterium*-mediated synthesis of selenium nanoparticles and their antifungal activity against *Rhizoctonia solani* in Faba bean plants. J. Fungi 7, 195. https://doi.org/10.3390/jof7030195.

Henry, G., Deleu, M., Jourdan, E., Thonart, P., Ongena, M., 2011. The bacterial lipopeptide surfactin targets the lipid fraction of the plant plasma membrane to trigger immune-related defence responses. Cell. Microbiol. 13, 1824–1837. https://doi.org/10.1111/j.1462-5822.2011.01664.x.

Horbach, R., Navarro-Quesada, A.R., Knogge, W., Deising, H.B., 2011. When and how to kill a plant cell: infection strategies of plant pathogenic fungi. J. Plant Physiol. 168, 51–62. https://doi.org/10.1016/j.jplph.2010.06.014.

Hutchinson, J.A., Burholt, S., Hamley, I.W., 2017. Peptide hormones and lipopeptides: from self-assembly to therapeutic applications. J. Pept. Sci. 23, 82–94. https://doi.org/10.1002/psc.2954.

Ibrahim, E., Zhang, M., Zhang, Y., Hossain, A., Qiu, W., Chen, Y., Wang, Y., Wu, W., Sun, G., Li, B., 2020. Green-synthesization of silver nanoparticles using endophytic bacteria isolated from garlic and its antifungal activity against wheat Fusarium head blight pathogen *Fusarium graminearum*. Nanomaterials 10 (2), 219 doi: 0.3390/nano10020219.

John, E., Singh, K.B., Oliver, R.P., Tan, K.-C., 2021. Transcription factor control of virulence in phytopathogenic fungi. Mol. Plant Pathol. 22, 858–881. https://doi.org/10.1111/mpp.13056.

Kim, Y.T., Kim, S.E., Lee, W.J., Fumei, Z., Cho, M.S., Moon, J.S., Oh, H.-W., Park, H.-Y., Kim, S.U., 2020. Isolation and characterization of a high iturin yielding *Bacillus velezensis* UV mutant with improved antifungal activity. PloS One 15, e0234177. https://doi.org/10.1371/journal.pone.0234177.

Li, S., Xu, J., Fu, L., Xu, G., Lin, X., Qiao, J., Xia, Y., 2022. Biocontrol of wheat crown rot using *Bacillus halotolerans* QTH8. Pathogens 11, 595. https://doi.org/10.3390/pathogens11050595.

Li, Z., Fernandez, K.X., Vederas, J.C., Gänzle, M.G., 2023. Composition and activity of antifungal lipopeptides produced by *Bacillus* spp. in daqu fermentation. Food Microbiol. 111, 104211 https://doi.org/10.1016/j.fm.2022.104211.

Lin, N., Wang, C., Ding, J., Su, L., Xu, L., Zhang, B., Zhang, Y., Fan, J., 2020. Efficacy of nanoparticle encapsulation on suppressing oxidation and enhancing antifungal activity of cyclic lipopeptides produced by *Bacillus subtilis*. Colloids Surf. B: Biointerfaces 193, 111143. https://doi.org/10.1016/j.colsurfb.2020.111143.

Malfanova, N., Franzil, L., Lugtenberg, B., Chebotar, V., Ongena, M., 2012. Cyclic lipopeptide profile of the plant-beneficial endophytic bacterium *Bacillus subtilis* HC8. Arch. Microbiol. 194, 893–899. https://doi.org/10.1007/s00203-012-0823-0.

Malviya, D., Sahu, P.K., Singh, U.B., Paul, S., Gupta, A., Gupta, A.R., Singh, S., Kumar, M., Paul, D., Rai, J.P., Singh, H.V., Brahmaprakash, G.P., 2020. Lesson from ecotoxicity: revisiting the microbial lipopeptides for the management of emerging diseases for crop protection. Int. J. Environ. Res. Public Health 17, 1434. https://doi.org/10.3390/ijerph17041434.

Masmoudi, F., Ben Khedher, S., Kamoun, A., Zouari, N., Tounsi, S., Trigui, M., 2017. Combinatorial effect of mutagenesis and medium component optimization on *Bacillus amyloliquefaciens* antifungal activity and efficacy in eradicating *Botrytis cinerea*. Microbiol. Res. 197, 29–38. https://doi.org/10.1016/j.micres.2017.01.001.

Masmoudi, F., Abdelmalek, N., Tounsi, S., Dunlap, C.A., Trigui, M., 2019. Abiotic stress resistance, plant growth promotion and antifungal potential of halotolerant bacteria from a Tunisian solar saltern. Microbiol. Res. 229, 126331 https://doi.org/10.1016/j.micres.2019.126331.

Meena, K.R., Kanwar, S.S., 2015. Lipopeptides as the antifungal and antibacterial agents: applications in food safety and therapeutics. Biomed. Res. Int. 2015, e473050 https://doi.org/10.1155/2015/473050.

Mezghanni, H., Khedher, S.B., Tounsi, S., Zouari, N., 2012. Medium optimization of antifungal activity production by *Bacillus amyloliquefaciens* using statistical experimental design. Prep. Biochem. Biotechnol. 42, 267–278. https://doi.org/10.1080/10826068.2011.614989.

Mittal, D., Kumar, A., Balasubramaniam, B., Thakur, R., Siwal, S.S., Saini, R.V., Gupta, R. K., Saini, A.K., 2022. Synthesis of biogenic silver nanoparticles using plant growth-promoting bacteria: potential use as biocontrol agent against phytopathogens. Biomater. Polym. Horizon 1, 22–31. https://doi.org/10.37819/bph.001.01.0130.

Mnif, I., Ghribi, D., 2015. Review lipopeptides biosurfactants: mean classes and new insights for industrial, biomedical, and environmental applications. Pept. Sci. 104, 129–147. https://doi.org/10.1002/bip.22630.

Mora, I., Cabrefiga, J., Montesinos, E., 2011. Antimicrobial peptide genes in *Bacillus* strains from plant environments. Int. Microbiol. 14, 213–223. https://doi.org/10.2436/20.1501.01.151.

Naseri, B., Marefat, A., 2011. Large-scale assessment of agricultural practices affecting *Fusarium* root rot and common bean yield. Eur. J. Plant Pathol. 131, 179–195. https://doi.org/10.1007/s10658-011-9798-y.

Panichikkal, J., Puthiyattil, N., Raveendran, A., Nair, R.A., Krishnankutty, R.E., 2021. Application of encapsulated *Bacillus licheniformis* supplemented with chitosan nanoparticles and rice starch for the control of *Sclerotium rolfsii* in *Capsicum annuum (L.)* seedlings. Curr. Microbiol. 78, 911–919. https://doi.org/10.1007/s00284-021-02361-8.

Pankaj, S.K., Shi, H., Keener, K.M., 2018. A review of novel physical and chemical decontamination technologies for aflatoxin in food. Trends Food Sci. Technol. 71, 73–83. https://doi.org/10.1016/j.tifs.2017.11.007.

Parveen, S., Wani, A.H., Shah, M.A., Devi, H.S., Bhat, M.Y., Koka, J.A., 2018. Preparation, characterization and antifungal activity of iron oxide nanoparticles. Microb. Pathog. 115, 287–292. https://doi.org/10.1016/j.micpath.2017.12.068.

Pillai, A.M., Sivasankarapillai, V.S., Rahdar, A., Joseph, J., Sadeghfar, F., Anuf, A.R., Rajesh, K., Kyzas, G.Z., 2020. Green synthesis and characterization of zinc oxide nanoparticles with antibacterial and antifungal activity. J. Mol. Struct. 1211, 128107 https://doi.org/10.1016/j.molstruc.2020.128107.

Price, N.P.J., Rooney, A.P., Swezey, J.L., Perry, E., Cohan, F.M., 2007. Mass spectrometric analysis of lipopeptides from *Bacillus* strains isolated from diverse geographical locations. FEMS Microbiol. Lett. 271, 83–89. https://doi.org/10.1111/j.1574-6968.2007.00702.x.

Rangarajan, V., Dhanarajan, G., Dey, P., Chattopadhya, D., Sen, R., 2018. *Bacillus* lipopeptides: powerful capping and dispersing agents of silver nanoparticles. Appl. Nanosci. 8, 1809–1821. https://doi.org/10.1007/s13204-018-0852-3.

Ravi, A., Nandayipurath, V.V.T., Rajan, S., Salim, S.A., Khalid, N.K., Aravindakumar, C. T., Krishnankutty, R.E., 2021. Effect of zinc oxide nanoparticle supplementation on the enhanced production of surfactin and iturin lipopeptides of endophytic *Bacillus sp*. Fcl1 and its ameliorated antifungal activity. Pest Manag. Sci. 77, 1035–1041. https://doi.org/10.1002/ps.6118.

Shi, J., Zhu, X., Lu, Y., Zhao, H., Lu, F., Lu, Z., 2018. Improving iturin A production of *Bacillus amyloliquefaciens* by genome shuffling and its inhibition against *Saccharomyces cerevisiae* in orangejuice. Front. Microbiol. 9.

Taheri, E., Tarighi, S., Taheri, P., 2023. An endophytic bacterium with biocontrol activity against important wheat pathogens. Biol. Control 183, 105243. https://doi.org/10.1016/j.biocontrol.2023.105243.

Tanaka, K., Amaki, Y., Ishihara, A., Nakajima, H., 2015. Synergistic effects of [Ile7] surfactin homologues with bacillomycin D in suppression of gray mold disease by *Bacillus amyloliquefaciens* biocontrol strain SD-32. J. Agric. Food Chem. 63, 5344–5353. https://doi.org/10.1021/acs.jafc.5b01198.

Toral, L., Rodríguez, M., Béjar, V., Sampedro, I., 2018. Antifungal activity of lipopeptides from *Bacillus* XT1 CECT 8661 against *Botrytis cinerea*. Front. Microbiol. 9.

Torres, M.J., Brandan, C.P., Petroselli, G., Erra-Balsells, R., Audisio, M.C., 2016. Antagonistic effects of *Bacillus subtilis* subsp. *subtilis* and *B. amyloliquefaciens* against *Macrophomina phaseolina*: SEM study of fungal changes and UV-MALDI-TOF MS analysis of their bioactive compounds. Microbiol. Res. 182, 31–39. https://doi.org/10.1016/j.micres.2015.09.005.

Trigui, M., Ben Hsouna, A., Hammami, I., Culioli, G., Ksantini, M., Tounsi, S., Jaoua, S., 2013. Efficacy of *Lawsonia inermis* leaves extract and its phenolic compounds against olive knot and crown gall diseases. Crop Prot. 45, 83–88. https://doi.org/10.1016/j.cropro.2012.11.014.

Umar, A., Zafar, A., Wali, H., Siddique, M.P., Qazi, M.A., Naeem, A.H., Malik, Z.A., Ahmed, S., 2021. Low-cost production and application of lipopeptide for bioremediation and plant growth by *Bacillus subtilis* SNW3. AMB Express 11, 165. https://doi.org/10.1186/s13568-021-01327-0.

Wildermuth, G.B., Thomas, G.A., Radford, B.J., McNamara, R.B., Kelly, A., 1997. Crown rot and common root rot in wheat grown under different tillage and stubble treatments in southern Queensland, Australia. Soil Tillage Res. 44, 211–224. https://doi.org/10.1016/S0167-1987(97)00054-8.

Wu, C.J., Li, C.W., Cui, C.B., 2014. Seven new and two known lipopeptides as well as five known polyketides: the activated production of silent metabolites in a marine-derived fungus by chemical mutagenesis strategy using diethyl sulphate. Mar. Drugs 12, 1815–1838. https://doi.org/10.3390/md12041815.

Xia, L., Wen, J., 2022. Available strategies for improving the biosynthesis of surfactin: a review. Crit. Rev. Biotechnol. 1–18 https://doi.org/10.1080/07388551.2022.2095252.

Yan, F., Li, C., Ye, X., Lian, Y., Wu, Y., Wang, X., 2020. Antifungal activity of lipopeptides from *Bacillus amyloliquefaciens* MG3 against Colletotrichum gloeosporioides in loquat fruits. Biol. Control 146, 104281. https://doi.org/10.1016/j.biocontrol.2020.104281.

Yánez-Mendizábal, V., Falconí, C.E., 2018. Efficacy of *Bacillus* spp. to biocontrol of anthracnose and enhance plant growth on Andean lupin seeds by lipopeptide production. Biol. Control 122, 67–75. https://doi.org/10.1016/j.biocontrol.2018.04.004.

Yaseen, Y., Diop, A., Gancel, F., Béchet, M., Jacques, P., Drider, D., 2018. Polynucleotide phosphorylase is involved in the control of lipopeptide fengycin production in *Bacillus subtilis*. Arch. Microbiol. 200, 783–791. https://doi.org/10.1007/s00203-018-1483-5.

Zhang, X., Yang, C.-W., Yu, H.-Q., Sheng, G.-P., 2016. Light-induced reduction of silver ions to silver nanoparticles in aquatic environments by microbial extracellular polymeric substances (EPS). Water Res. 106, 242–248. https://doi.org/10.1016/j.watres.2016.10.004.

Zhao, J., Cao, L., Zhang, C., Zhong, L., Lu, J., Lu, Z., 2014. Differential proteomics analysis of *Bacillus amyloliquefaciens* and its genome-shuffled mutant for improving surfactin production. Int. J. Mol. Sci. 15, 19847–19869. https://doi.org/10.3390/ijms151119847.

Zhao, X., Yan, L., Xu, X., Zhao, H., Lu, Y., Wang, Y., Jiang, C., Shao, D., Zhu, J., Shi, J., 2019. Synthesis of silver nanoparticles and its contribution to the capability of *Bacillus subtilis* to deal with polluted waters. Appl. Microbiol. Biotechnol. 103, 6319–6332. https://doi.org/10.1007/s00253-019-09880-2.

Zouari, I., Masmoudi, F., Medhioub, K., Tounsi, S., Trigui, M., 2020. Biocontrol and plant growth-promoting potentiality of bacteria isolated from compost extract. Antonie Van Leeuwenhoek 113, 2107–2122. https://doi.org/10.1007/s10482-020-01481-8.